5-1-2018

NMR studies of the helical antiferromagnetic compound EuCo2P2

N. Higa
Ames Laboratory

Qing-Ping Ding
Ames Laboratory, ding@ameslab.gov

F. Kubota
University of the Ryukyus

H. Uehara
University of the Ryukyus

M. Yogi
University of the Ryukyus

See next page for additional authors

NMR studies of the helical antiferromagnetic compound EuCo2P2

Abstract
In EuCo2P2, 4f electron spins of Eu2+ ions order antiferromagnetically below a Néel temperature . The magnetic structure below was reported to be helical with the helix axis along the c-axis from the neutron diffraction study. We report the results of 153Eu, 59Co and 31P nuclear magnetic resonance (NMR) measurements on EuCo2P2 using a single crystal and a powdered sample. In the antiferromagnetic (AFM) state, we succeeded in observing 153Eu, 59Co and 31P NMR spectra in zero magnetic field. The sharp 153Eu zero field NMR (ZF NMR) lines indicate homogeneous Eu ordered moment. The 59Co and 31P ZF NMR spectra showed an asymmetric spectral shape, indicating a distribution of the internal magnetic induction at each nuclear position. The AFM propagation vector k characterizing the helical AFM state can be determined from the internal magnetic induction at Co site. We have determined the model-independent value of the AFM propagation vector k distributed from $(0, 0, 0.86)2\pi/c$ to $(0, 0, 0.73)2\pi/c$, where c is the lattice parameter.

Keywords
EuCo2P2, Helical antiferromagnet, Antiferromagnetic propagation vector, NMR

Disciplines
Condensed Matter Physics | Materials Science and Engineering | Metallurgy

Authors
N. Higa, Qing-Ping Ding, F. Kubota, H. Uehara, M. Yogi, Yuji Furukawa, N. S. Sangeetha, David C. Johnston, A. Nakamura, M. Hedo, T. Nakama, and Y. Onuki

NMR studies of the helical antiferromagnetic compound $EuCo_2P_2$

N. Higa[a,b,*], Q.-P. Ding[a], F. Kubota[b], H. Uehara[b], M. Yogi[c], Y. Furukawa[a], N. S. Sangeetha[a], D. C. Johnston[a], A. Nakamura[d], M. Hedo[c], T. Nakama[c], Y. Ōnuki[c]

[a] *Ames Laboratory, U.S. DOE, and Department of Physics and Astronomy, Iowa State University, Ames, Iowa 50011, USA*
[b] *Graduate School of Engineering and Science, Univesity of the Ryukyus, Nishihara, Okinawa 903-0213, Japan*
[c] *Faculty of Science, Univesity of the Ryukyus, Nishihara, Okinawa 903-0213, Japan*
[d] *Institute for Materials Research, Tohoku University, Oarai, Ibaraki 319-1195, Japan*

Abstract

In $EuCo_2P_2$, $4f$ electron spins of Eu^{2+} ions order antiferromagnetically below a Néel temperature $T_N = 66.5$ K. The magnetic structure below T_N was reported to be helical with the helix axis along the c-axis from the neutron diffraction study. We report the results of ^{153}Eu, ^{59}Co and ^{31}P nuclear magnetic resonance (NMR) measurements on $EuCo_2P_2$ using a single crystal and a powdered sample. In the antiferromagnteic (AFM) state, we succeeded in observing ^{153}Eu, ^{59}Co and ^{31}P NMR spectra in zero magnetic field. The sharp ^{153}Eu zero field NMR (ZF-NMR) lines indicate homogeneous Eu ordered moment. The ^{59}Co and ^{31}P ZF-NMR spectra showed an asymmetric spectral shape, indicating a distribution of the internal magnetic induction at each nuclear position. The AFM propagation vector **k** characterizing the

*Corresponding author
Email address: k158652@eve.u-ryukyu.ac.jp (N. Higa)

helical AFM state can be determined from the internal magnetic induction at Co site. We have determined the model-independent value of the AFM propagation vector **k** distributed from (0, 0, 0.86)$2\pi/c$ to (0, 0, 0.73)$2\pi/c$, where c is the lattice parameter.
Keywords: $EuCo_2P_2$, helical antiferromagnet, antiferromagnetic propagation vector, NMR

1. Introduction

Understanding of the interplay between $4f$ and conduction electrons in intermetallic compounds has been one of the important issues in strongly correlated electron systems. Eu is a rare-earth element known to have two kinds of valence state. The divalent Eu state Eu^{2+} ($4f^6$) is magnetic ($J = S = 7/2$, $L = 0$), where J is the total angular momentum, S is the spin angular momentum, and L is the orbital angular momentum. Therefore, the compounds with divalent Eu ions tend to order magnetically, following the Ruderman-Kittel-Kasuya-Yosida (RKKY) interaction. In contrast, the trivalent Eu state Eu^{3+} ($4f^7$) is non-magnetic ($J = 0$, $S = L = 3$).

The Eu-based intermetallic compound $EuCo_2P_2$ crystallizes in the $ThCr_2Si_2$-type structure (Space group: No. 139, $I4/mmm$, D_{4h}^{17}) as shown in Fig. 1. In $EuCo_2P_2$, Eu ion has the divalent state, and orders antiferromagnetically below the Néel temperature $T_N = 66.5$ K [1, 2, 3, 4, 5]. The ordered magnetic moment was reported to be 6.9 μ_B/Eu at 15 K, which is close to 7 μ_B/Eu expected for the Eu^{2+} spins. The antiferromagnetic (AFM) structure below T_N was reported to be helical as shown in Fig. 1 from the neutron diffraction (ND) study [1]. The Eu ordered moments are aligned ferromagnetically in

the *ab*-plane with the helix axis along the *c*-axis [1].

Nuclear magnetic resonance (NMR) measurement is useful for determination of the magnetic structure in AFMs such as high-T_c cuprates and Fe-based superconductors. However, it is usually difficult to determine its AFM propagation vector in helical antiferromagnets from NMR measurements alone. Quite recently, the AFM propagation vector of the incommensurate helical state in $EuCo_2As_2$ below $T_N \sim 45$ K [6, 7], which has the same crystal structure as that of $EuCo_2P_2$, was successfully determined by using NMR [8]. This result indicates NMR is another unique tool to determine the spin structure in incommensurate helical AFM state.

Here, we carried out zero magnetic field NMR (ZF-NMR) measurements to elucidate the spin structure in the incommensurate helical AFM state on $EuCo_2P_2$. We succeeded in observing NMR signals from all three ^{153}Eu, ^{59}Co and ^{31}P nuclei. From the analysis of the observed spectra, we determined the helical structure and the AFM propagation vector $\mathbf{k}$.

2. Experimental

A single crystal of $EuCo_2P_2$ was grown by Sn flux method. Details of the sample preparation are described elsewhere [2, 5]. ZF-NMR measurements were performed on ^{153}Eu ($I = 5/2$, $\gamma_N/2\pi = 4.632$ MHz/T, $Q = 2.49$ barns), ^{59}Co ($I = 7/2$, $\gamma_N/2\pi = 10.03$ MHz/T, $Q = 0.4$ barns), and ^{31}P ($I = 1/2$, $\gamma_N/2\pi = 17.235$ MHz/T) nuclei, respectively. We used a single crystal only for ^{153}Eu ZF-NMR spectrum measurement at the lowest temperature of 1.6 K. Because the signal intensity of the single crystal is weak, the powdered samples were used to measure the temperature dependence of ^{59}Co and

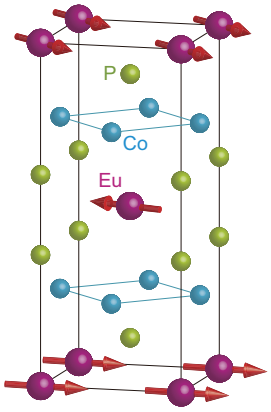

Figure 1: (Color online) Crystal and magnetic structures of $EuCo_2P_2$.

^{31}P ZF-NMR, spectra. The ZF-NMR spectra were obtained by sweeping the frequency and integrating the spin-echo signal intensity step by step.

3. Results and discussion

Figure 2 shows the ^{153}Eu ZF-NMR spectrum in the AFM state for $EuCo_2P_2$ measured at a temperature $T = 1.6$ K. The observed ^{153}Eu ZF-NMR spectrum is well reproduced by the following simple nuclear spin Hamiltonian given by

$$\mathcal{H} = -\gamma_{\rm N}\hbar\mathbf{I}\cdot\mathbf{B}_{\rm int} + \frac{h\nu_{\rm Q}}{6}[3I_z^2 - I(I+1) + \frac{1}{2}\eta(I_+^2 + I_-^2)]. \qquad (1)$$

The first term represents the Zeeman interaction, where $\gamma_{\rm N}$ is the nuclear gyromagnetic ratio, I is the nuclear spin and $B_{\rm int}$ is the internal magnetic induction at the Eu site. The second term corresponds to the nuclear quadrupole interaction between the electric field gradient (EFG) and the nuclear quadrupole moment Q. Here, ν_Q is the nuclear quadrupole frequency defined as $\nu_Q \equiv$

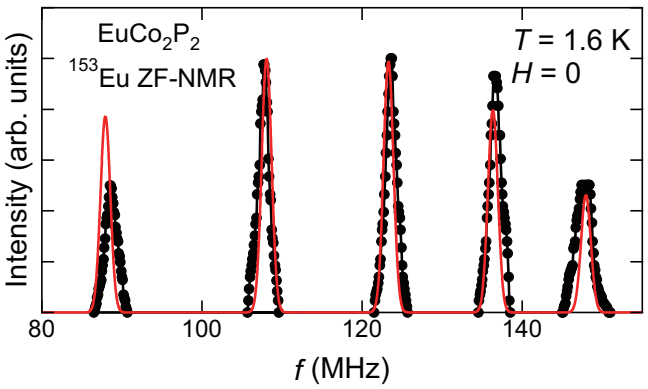

Figure 2: (Color online) ^{153}Eu-NMR spectrum at T = 1.6 K in the AFM state for the single crystalline $EuCo_2P_2$ in $H = 0$. The solid line is the calculated ^{153}Eu NMR spectrum.

$3eQV_{zz}/2I(2I-1)h$ ($=3e^2QV_{ZZ}/20h$ for $I = 5/2$), V_{zz} is the main principal axis of the EFG and parallels to the c-axis, and η is the asymmetry parameter of EFG [9]. In $EuCo_2P_2$, η is zero because of the axially symmetric EFG at each nuclear site. The obtained ^{153}Eu NMR spectrum was analyzed using the Hamiltonian in Eq. (1). The solid line as shown in Fig. 2 is the calculated ^{153}Eu ZF-NMR resonance lines with the parameters $|B_{\rm int}^{\rm Eu}|$ = 25.75(2) T, $\nu_{\rm Q}$ = 30.2(2) MHz and $\theta = 90°$. Here θ represents the angle between $B_{\rm int}^{\rm Eu}$ and the principal axis of the EFG tensor at the Eu sites. The obtained values are similar to the case of the ^{153}Eu nuclei in $EuCo_2As_2$ and $EuGa_4$ in which $B_{\rm int}^{\rm Eu}$ = 27.5 T and $\nu_{\rm Q}$ = 30.6 MHz, and $B_{\rm int}^{\rm Eu}$ = 27.08 T and $\nu_{\rm Q}$ = 30.5 MHz, respectively [8, 10].

We have succeeded in observing the ^{59}Co ZF-NMR spectrum below 30 K as shown in Fig. 3(a). For $I = 7/2$ nuclei, the NMR Hamiltonian [Eq.(1)] produces a spectrum with a sharp central transition line flanked by three satellite peaks on both sides. However, the observed ^{59}Co ZF-NMR spec-

tra do not show the seven distinct lines and rather show one peak with the asymmetric shape. The homogeneous Eu ordered moment has been exhibited from the sharp ^{153}Eu ZF-NMR lines. Therefore, we assume that the asymmetric shape of ^{59}Co ZF-NMR spectra is due to the contribution of internal magnetic induction $|B_{\rm int}^{\rm Co}|$ at the Co site. According to the analysis performed in $EuCo_2As_2$ [8], one can estimate the AFM propagation vector in the incommensurate state of $EuCo_2P_2$ with the estimated values of $|B_{\rm int}^{\rm Co}|$ and the hyperfine coupling constant at Co site $A^{\rm Co}$. The internal magnetic induction at the Co site is expressed by

$$B_{\rm int}^{\rm Co} = 2\langle\mu\rangle A^{\rm Co}\sqrt{2+2\cos\phi}, \tag{2}$$

where $\langle\mu\rangle$ is the Eu ordered moment, and ϕ is the turn angle between the Eu ordered moments on adjacent Eu planes along the c-axis, which characterizes the helical structure [8]. In the case of $\phi = \pi$ corresponding to an A-type collinear AFM state, $B_{\rm int}^{\rm Co}$ is zero due to a cancellation of the internal magnetic induction from the four nearest-neighbor Eu ordered moments. On the other hand, if ϕ deviates from π corresponding to a helical state, one can expect a finite $B_{\rm int}^{\rm Co}$. Since the distance (d) along the c-axis between adjacent layers of ferromagnetic-aligned Eu moments is $d = c/2$, the turn angle between the ordered moments in adjacent Eu layers is $\phi = kd$, as shown in Fig. 3(b). Using the values of $\langle\mu\rangle = 6.9(1)$ $\mu_{\rm B}$, $A^{\rm Co} = -0.98$ kOe/$\mu_{\rm B}$/Eu (obtained from ^{59}Co NMR measurement in the paramagnetic state [11]), and the internal magnetic induction distribution of the Co site from 6 kOe (6 MHz) to 12 kOe (12 MHz) at 1.6 K, the turn angle ϕ is estimated to be from 156° to 131°. These correspond to helix wave vector $\mathbf{k}$ from (0, 0, 0.86)$2\pi/c$ to

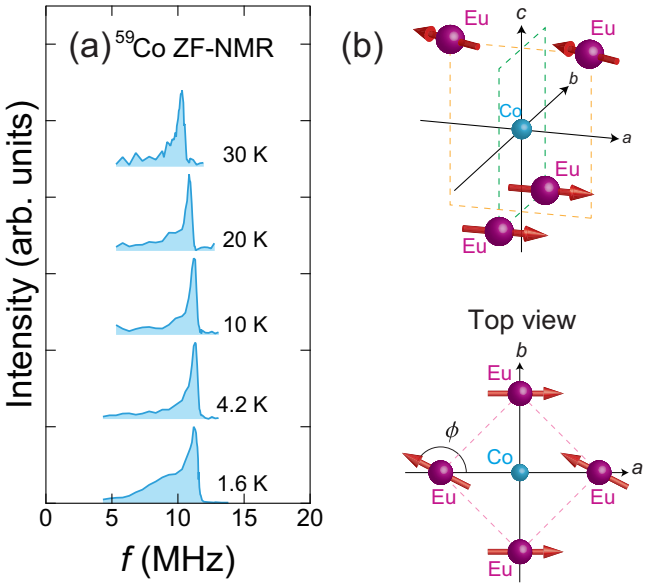

Figure 3: (Color online) (a) ^{59}Co ZF-NMR spectrum at various temperatures in the AFM state at zero magnetic field. (b) The coordination of nearest-neighbor Eu sites around Co site. The arrows on the Eu atoms indicate the magnetic moment. The magnetic moment turn angle between adjacent magnetic layers is ϕ.

(0, 0, 0.73)$2\pi/c$. These $\mathbf{k}$ values are close to $\mathbf{k}$ = (0, 0, 0.852(4))$2\pi/c$ and (0, 0, 0.88)$2\pi/c$ obtained from ND data [1] and χ measurement [5], respectively. The temperature dependence of the distribution of $|B_{\rm int}^{\rm Co}|$ is shown in Fig. 4(a). Using the data, we estimated the temperature dependence of the distribution of ϕ as shown in Fig. 4(b). Although the result of ND measurements indicates the change of ϕ from 150° at 64 K just below $T_{\rm N}$ to 153° at 15 K [1], we did not observe a clear change in $\mathbf{k}$ up to 30 K within our experimental uncertainty.

Figure 5(a) shows the ^{31}P ZF-NMR spectra at various temperatures in the AFM state. The spectra shift to lower frequency side with increasing

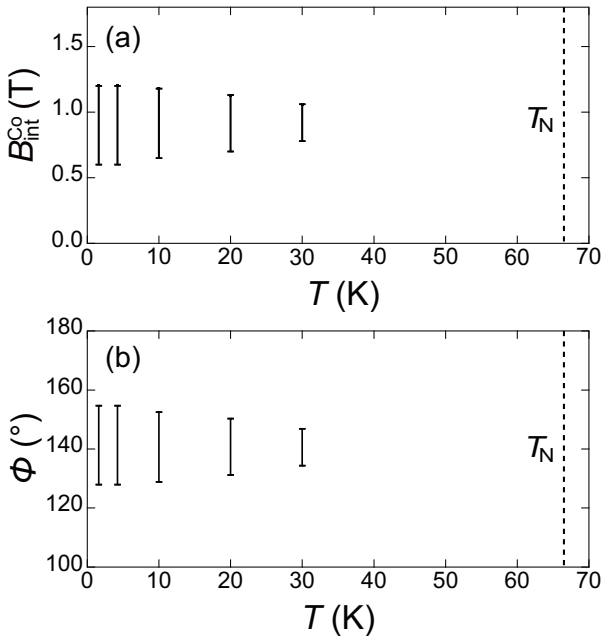

Figure 4: (Color online) (a) Temperature dependence of $B_{\rm int}^{\rm Co}$. (b) Temperature dependence of ϕ.

temperature as shown in the inset of Fig. 5(b). The internal magnetic induction $|B_{\rm int}^{\rm P}|$, estimated from a peak position of the spectrum, is shown in Fig. 5(b). The temperature dependence of $|B_{\rm int}^{\rm P}|$ is well explained by a Brillouin function which is calculated based on the Weiss molecular field model with $J = S = 7/2$, $T_{\rm N} = 66.5$ K, and $B_{\rm int}^{\rm P} = 2.69$ T at $T = 1.6$ K. This result indicates that the divalent Eu ion is stable and the magnetic state is well explained by the local moment picture in $EuCo_2P_2$.

Because of no nuclear quadrupole interaction for $I = 1/2$ nucleus, a single NMR line is expected for ^{31}P ZF-NMR. However, the ^{31}P ZF-NMR spectrum showed complex structure at low temperature below 10 K as shown in Fig. 5(a). The spectrum shape shows clear temperature dependence and

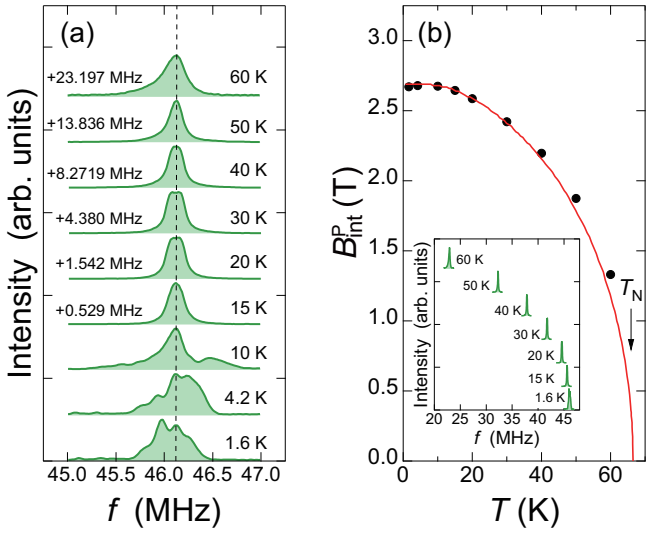

Figure 5: (Color online) (a) ^{31}P ZF-NMR spectrum using powdered sample at various temperatures in the AFM state for $EuCo_2P_2$ in zero magnetic field. Above 15 K, we shift frequency to compare the shape of spectra. (b) Temperatures dependence of $B_{\rm int}^{\rm P}$. The solid line is the Brillouin function with $J = S = 7/2$. The inset shows the temperature dependence of ^{31}P ZF-NMR spectra.

becomes almost symmetrical shape above 10 K. The complex ^{31}P ZF-NMR spectrum shape shows a distribution of the internal magnetic induction at the P site. If we consider only the contribution by the nearest-neighbor (NN) Eu ions to the P site, the internal magnetic induction does not depend on the **k** vector. Therefore, it is necessary to take into account the contribution of the next-nearest-neighbor (NNN) Eu site. Figure 6 indicates the configuration of the NN and the NNN Eu ions around the P site. If the contribution to the internal magnetic induction by the NNN is comparably small compared to the NN, the total magnetic induction at the P site can be written as

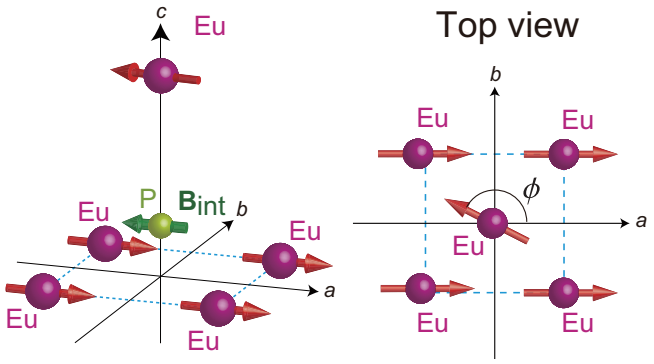

Figure 6: (Color online) The coordinations of nearest-neighbor and next-nearest-neighbor Eu sites around the P site. The arrows on the Eu and P atoms indicate the directions of the Eu ordered moment and the internal magnetic induction at the P site, respectively.

$$B_{\rm int}^{\rm P} = B_{\rm int}^{\rm NN} + B_{\rm int}^{\rm NNN} \cos\phi. \tag{3}$$

Here, $B_{\rm int}^{\rm NN}$ and $B_{\rm int}^{\rm NNN}$ are the internal magnetic induction by the NN and the NNN Eu ions, respectively. Since the magnitude of the internal magnetic inductions is proportional to the resonance frequency, the complicated spectrum shape means a distribution of the internal magnetic induction, that is, the distribution of the **k** vector, which is suggested from not only ^{59}Co ZF-NMR but also ^{31}P ZF-NMR. Since the distribution of **k** is not observed in the ND measurement, an origin of the distribution is presumed to be due to distortions in the crystal due to powdering.

4. Conclusions

We succeeded in observing the ^{153}Eu, ^{59}Co, and ^{31}P ZF-NMR spectra on the helical antiferromagnet $EuCo_2P_2$ with $T_{\rm N} = 66.5$ K. The sharp ^{153}Eu

ZF-NMR lines indicate a homogeneous Eu ordered moment. The AFM propagation vector characterizing the incommensurate helical AFM state was determined from the internal magnetic induction at the Co cite. The internal magnetic induction shows a distribution, i.e., the AFM propagation vector distributes from (0, 0, 0.86)$2\pi/c$ to (0, 0, 0.73)$2\pi/c$. The distribution of the AFM propagation vector is also observed in the ^{31}P ZF-NMR spectrum. The distribution of the internal magnetic inductions at Co and P sites may be caused by powdering the sample which introduces distortions.

Acknowledgments

The research was supported by the U.S. Department of Energy, Office of Basic Energy Sciences, Division of Materials Sciences and Engineering. Ames Laboratory is operated for the U.S. Department of Energy by Iowa State University under Contract No. DE-AC02-07CH11358. Part of the work was supported by the Japan Society for the Promotion of Science KAKENHI: J-Physics (Grant Nos. JP15K21732, JP15H05885, and JP16H01078). N. H. also thanks the KAKENHI: J-Physics for financial support to be a visiting scholar at the Ames laboratory.

[1] M. Reehuis, W. Jeitschko, M. H. Möller, and P. J. Brown, A neutron diffraction study of the magnetic structure of $EuCo_2P_2$, J. Phys. Chem. Solids **53**, 687 (1992).

[2] R. Marchand and W. Jeitschko, Ternary lanthanoid-transition metal pnictides with $ThCr_2Si_2$-type structure, J. Solid State Chem. **24**, 351 (1978).

[3] E. Mörsen, B. D. Mosel, W. Müller-Warmuth, M. Reehuis, and W. Jeitschko, Mössbauer and magnetic susceptibility investigations of strontium, lanthanum and europium transition metal phosphides with $ThCr_2Si_2$ type structure, J. Phys. Chem. Solids **49**, 785 (1988).

[4] T. Nakama, T. Yoshida, A. Ohno, D. Nakamura, Y.Takaesu, M. Hedo, K. Yagasaki, K. Uchima, T. Fujiwara, and T. Shigeoka, Effect of pressure on thermopower and resistivity of $EuCo_2P_2$, J. Phys.: Conf. Ser. **200**, 032050 (2010).

[5] N. S. Sangeetha, E. Cuervo-Reyes, A. Pandey, and D. C. Johnston, $EuCo_2P_2$:A model molecular-field helical Heisenberg antiferromagnet, Phys. Rev. B **94**, 014422 (2016).

[6] H. Raffius, E. Mörsen, B. D. Mosel, W. Müller-Warmuth, W. Jeitschko, L. Terbüchte, and T. Vomhof, Magnetic properties of ternary lanthanoid transition metal arsenides studied by Mössbauer and susceptibility measurements, J. Phys. Chem. Solids **54**, 135 (1993).

[7] J. ballinger, L. E. Wenger, Y. K. Vohra, and A. S. Sefat, Magnetic properties of single crystal $EuCo_2As_2$, J. Appl. Phys. **111**, 07E106 (2012).

[8] Q.-P. Ding, N. Higa, N. S. Sangeetha, D. C. Johnston, and Y. Furukawa, NMR determination of an incommensurate helical antiferromagnetic structure in $EuCo_2As_2$, Phys. Rev. B **95**, 184404 (2017).

[9] C. P. Slichter, *Principles of Magnetic Resonance*, 3rd ed. (Springer, New York, 1990).

[10] M. Yogi, S. Nakamura, N. Higa, H. Niki, Y. Hirose, Y. Ōnuki, and H. Harima, ^{153}Eu and ^{69,71}Ga zero-field NMR study of antiferromagnetic state in $EuGa_4$, J. Phys. Soc. Jpn. **82**, 103701 (2013).

[11] N. Higa, Q.-P. Ding, M. Yogi, N. S. Sangeetha, M. Hedo, T. Nakama, Y. Ōnuki, D. C. Johnston, and Y. Furukawa, NMR studies of the incommensurate helical antiferromagnet $EuCo_2P_2$: Determination of antiferromagnetic propagation vector, Phys. Rev. B **96**, 024405 (2017).